A CONUS-Wide Standardized Precipitation–Evapotranspiration Index for Major U.S. Row Crops

PETER E. GOBLE,[a,b] REBECCA A. BOLINGER,[a,b] AND RUSS S. SCHUMACHER[a,b]

[a]*Department of Atmospheric Science, Colorado State University, Fort Collins, Colorado*
[b]*Colorado Climate Center, Fort Collins, Colorado*

(Manuscript received 13 November 2020, in final form 23 August 2021)

ABSTRACT: Agricultural droughts afflicting the contiguous United States (CONUS) are serious and costly natural hazards. Widespread damage to a single cash crop may be crippling to rural communities that produce it. While drought is insidious in nature, drought indices derived from meteorological data and drought impact reports both provide essential guidance to decision-makers about the location and intensity of developing and ongoing droughts. However, response to dry meteorological conditions is not consistent from one crop type to the next, making crop-specific drought appraisal difficult using weather data alone. Additionally, drought impact reports are often subjective, latent, or both. To rectify this, we developed drought indices using meteorological data, and phenological information for the row crops most commonly grown over CONUS: corn, soybeans, and winter wheat. These are referred to as crop-specific standardized precipitation–evapotranspiration indices (CSPEIs). CSPEIs correlate more closely with end-of-season yields than traditional meteorological indicators for the eastern two thirds of CONUS for corn, and offer an advantage in predicting winter wheat yields for the High Plains. CSPEIs do not always explain a higher fraction of variance than traditional meteorological indicators. In such cases, results provide insight on which meteorological indicators to use to most effectively supplement impacts information.

SIGNIFICANCE STATEMENT: This manuscript is expected to advance the science of drought monitoring and appraisal over CONUS. Using gridded weather data and a novel framework for assessing meteorological conditions over major U.S. row crops, we gain an improved understanding of the conditions leading to most severe agricultural drought impacts.

KEYWORDS: Climate variability; Evapotranspiration; Hydrology; Hydrometeorology

1. Introduction

Drought is a costly natural hazard with far-reaching societal impacts. Recent major droughts, such as the 2011 Southern Plains Drought, 2012 Central Plains Drought, California Megadrought, and 2017 Northern Plains Drought, have all resulted in multibillion dollar economic losses (Smith 2020). Drought poses risk to water supply (e.g., Wilhite et al. 2005; Udall and Overpeck 2017; Sousa et al. 2018), and food security (e.g., Al-Kaisi et al. 2013; Lesk et al. 2016). Droughts can cause mental health complications or exacerbate existing ones (Vins et al. 2015). Historic droughts have resulted in mass migrations (e.g., Benson et al. 2006), and even provoked, or escalated human conflict (e.g., Selby et al. 2017). Droughts are expected to develop more rapidly and become more intense as the climate continues to warm (Pendergrass et al. 2020; Trenberth et al. 2014). All these factors illustrate the need for timely and accurate drought warning and detection capabilities.

Improving overall drought monitoring is onerous because there is no universally accepted definition of drought (Belal et al. 2014). Put simply, drought is "insufficient water to meet needs" (Redmond 2002). Drought is a unique hazard. While most weather-driven disasters are measured primarily using weather data (e.g., Groisman et al. 2004; Emanuel 2005; Perkins and Alexander 2013), drought severity is determined using impact data as guidance. To this point, the *Glossary of the Meteorology* (American Meteorological Society 2020) states "drought is a relative term, therefore any discussion in terms of precipitation must refer to the particular precipitation-related activity that is under discussion." Otherwise stated by Dr. Kelly Redmond, "Drought is a many-headed creature, and its full description requires an equally diverse menagerie of indices and indicators" (Redmond 2002). Definitions of drought vary based on both time scale and sector. For instance, a flash drought is one of rapid onset, defined by speed of degradation of soil and vegetation conditions (Otkin et al. 2018). Conversely, longer sustained droughts may both develop more slowly, but lead to serious, and long-lasting hydrological imbalances [e.g., Dust Bowl Drought (Schubert et al. 2004) and California Megadrought (Kwon and Lall 2016)]. A set of meteorological conditions will produce impacts of varying severity across different drought-affected sectors (e.g., agricultural, hydrological, ecological, recreational) (Redmond 2002).

Our focus in this study is on agricultural drought. We implement a novel approach to appraising droughts over common U.S. row crops by computing crop-specific standardized precipitation–evaporation indices (CSPEIs) over the entire contiguous United States (CONUS) from 1980 to present.

Corresponding author: Peter Goble, peter.goble@colostate.edu

DOI: 10.1175/JHM-D-20-0270.1

These indices are designed with operational usage during the growing season in mind.

One well-known source for drought information is the National Drought Mitigation Center (NDMC). The NDMC, along with several partnering federal offices around the country, has produced a single, nationwide map of drought conditions every week since 2000 (Lawrimore et al. 2002). The U.S. Drought Monitor map is not explicitly an agricultural drought product but is tied to billions of dollars of agricultural federal disaster relief funding (Rippey 2019). Improvement of the product is called for explicitly in the current United States Farm Bill (House of Representatives 2018).

Given the nature of agricultural drought, collecting accurate drought impact data is key to successful appraisal of severity. Concerted efforts to monitor drought impacts do exist nationally. One such effort is the National Drought Mitigation Center's Drought Impact Reporter, a tool that aggregates drought impact information from the media and the public (Smith et al. 2014). The U.S. Drought Monitor's weekly update process allows for communication with experts across the country. These experts range from State Climate Offices to National Weather Service Employees to Regional Climate Centers and other state and federal entities. Each week experts share impacts being experienced on local, state, and regional scales with the Drought Monitor. Another technique used to gather impacts data is to crowd source them via community scientists. The Community Collaborative Rain, Hail and Snow Network (CoCoRaHS) gathers such reports from volunteer rainfall reporters (Lackstrom et al. 2017; Reges et al. 2016). Despite the human communication infrastructure associated with tracking agricultural drought, and drought impacts, there is a need for quantitative, objective metrics designed to accurately depict conditions.

A plethora of indicators and indices have been developed to measure agricultural drought. These indicators span diverse methodology and data source material. The first effort, which is still used today, was the Palmer drought severity index (PDSI) developed in 1965 (Palmer 1965). This drought indicator initially used weather station temperature and precipitation data to estimate available soil moisture (Alley 1984). It has been adapted in numerous ways including but not limited to the following: making the index multiscalar (Liu et al. 2017), adapting the PDSI to different types of drought (Alley 1985), restandardizing the index, and creating gridded adaptations of the product (Abatzoglou et al. 2017).

Mulitscalar drought indices that allow for computation of surface water balance fluxes are useful in the agricultural sector. These indicators are adaptable to the time scales on which agricultural conditions evolve, which are seasonally, spatially, and operationally variable. Examples of such products include the standardized precipitation index (SPI) (McKee et al. 1993), evaporative demand drought index (EDDI) (Hobbins et al. 2016), and standardized precipitation–evapotranspiration index (SPEI) (Beguería et al. 2014). The SPI addresses precipitation (P) only, EDDI addresses reference evapotranspiration (ET_r) only, and the SPEI addresses both precipitation and potential evapotranspiration (PET).

A considerable amount of effort has been put into developing soil moisture indicators to address agricultural drought. This includes leveraging agricultural weather station data (e.g., Scott et al. 2013), national observation networks (Schaefer et al. 2007), remote sensing products (Entekhabi et al. 2010), and modeling products (Xia et al. 2014). Efforts to track soil moisture for drought monitoring purposes are explicitly addressed in South Dakota Senator John Thune's amendment to the United States Farm Bill (House of Representatives 2018). An ongoing effort to establish a National Coordinated Soil Moisture Monitoring Network that compiles soil moisture drought indicators is also underway (Quiring et al. 2015; Clayton et al. 2019).

A variety of satellite-based agricultural drought indicators have been created: the vegetation drought response index (VegDRI) measures anomalies in the ratio of reflected and absorbed near-infrared sunlight (Brown et al. 2008). When near-infrared radiation is absorbed at lower-than-normal rates, it is indicative of less photosynthetic activity, which indicates drought stress. Others use satellite data to derive actual evapotranspiration (AET) (Otkin et al. 2013; Rangwala et al. 2019), and compute anomalies of either AET (Rangwala et al. 2019), or the ratio AET/PET (Otkin et al. 2013). Many of these have been developed recently, following the central plains drought of 2012, a multi-billion-dollar disaster with major agricultural impacts (Rippey 2015; Smith 2020).

All of these indices come with known strengths and weaknesses, and the most appropriate indicators for usage vary based on application (Svoboda and Fuchs 2016). What existing, popularized, CONUS-wide, agricultural drought indicators do not provide is information designed to track drought severity over a specific cash crop. Such information is vital as a single cash crop may be the driving force behind a local, or regional economy, and control the narrative of a given drought.

Despite the myriad of indicators available, drought is still largely defined by its impacts. For much of the CONUS, notably the central, intercontinental portions of CONUS, community-level drought impacts will be determined by the impact to cash crops. Efforts to quantify impacts to cash crops do exist, but data are not available for weeks, or sometimes months, after damages are realized (NASS 2020b). Qualitative assessments, such as those available through the Drought Impact Reporter and CoCoRaHS Condition Monitoring, sometimes provide valuable crop-specific drought impact information. However, there are disadvantages to relying upon qualitative information alone. Even if one assumes these reports are gathered by trained, unbiased observers, they are impossible to standardize. What looks like "moderate drought" to one observer may appear "severe" to another. We recommend supplementing impact reports with a drought indicator with the following features:

(i) data driven, subject to as little bias as possible;
(ii) accurately characterizes the crop being modeled;
(iii) strongly related to current and or future agricultural impacts;

(iv) computed using real-time data with weekly, or finer, temporal resolution; and
(v) covers the United States with high spatial resolution.

In this study, we created such indicators for corn, soybeans, and winter wheat. These indicators rank water balance for each crop in each year from planting date to harvest similarly to the SPEI (Beguería et al. 2014). The key difference is evapotranspiration is computed based on crop type. In so doing, the following questions are answered: 1) Do CSPEIs correlate more closely with the yields of the crops they model than traditional meteorological drought indicators? 2) At what point in the growing season does a statistically significant relationship materialize, and does it hold through the remainder of the growing season?

Efforts to derive crop-specific drought indices have been conducted before on regional scales and have shown promise. For instance, crop-specific SPEIs were computed for several field crops on the Texas high plains, and correlated more closely with end-of-season yields than traditional drought indicators (Moorhead et al. 2013). A corn-specific index has been used with success to predict yields in eastern Nebraska (Meyer et al. 1993a,b). The effort demonstrated here, however, is unprecedented in spatial and temporal scale, and intended for operational drought monitoring usage.

2. Methods

CSPEIs are computed for corn, soybeans, and winter wheat for every day of the growing season for every year from 1980 to 2019. We then investigate the relationship between these indices and yields at county scale. We investigate at what level CSPEIs are indicative of optimal yields, and the correlation between CSPEI and yields for drier than normal growing season (CSPEI < 0). The same correlation analysis procedure is followed with a suite of traditional drought indicators: SPI (McKee et al. 1993), EDDI (Hobbins et al. 2016), and SPEI (Beguería et al. 2014) on a bimonthly basis at time scales of 1, 3, 6, 9, and 12 months. In total, this is 360 unique drought indicators. Special attention is paid to the comparison between end of model-parameterized growing season (MPGS) CSPEs, and SPIs, EDDIs, and SPEIs (traditional indicators) of a 6-month aggregation period, as this is most similar to growing season length. If full growing season CSPEIs correlate more closely to yields than most, or all, traditional indicators, they may improve agricultural drought monitoring. Furthermore, the sooner in the growing season these correlations become robust, the more potential early warning of agricultural drought impacts.

The methodology prescribed herein is flexible and may be appropriate for many crops. The crops chosen for evaluation were corn, soybeans, and winter wheat. These crops were chosen due to their production scale over CONUS. Corn, soybeans, and wheat are the three most planted crops by area in the United States with 89.7, 76.5, and 31.2 million acres planted, respectively, in 2019 (NASS 2020a).

a. Data

Temperature, precipitation, and potential evapotranspiration data used in this study were obtained from North American Land Data Assimilation Systems (NLDAS) Forcing "A" (Rui and Mocko 2019). This dataset assimilates observations from surface weather stations, satellites, radiosondes, dropsondes, and aircraft to reconstruct weather conditions across North America on a 12-km grid. Precipitation data are gauge data interpolated using climatology from the Parameterized Regression on Independent Slopes Model (PRISM) (Daly et al. 2008; Rui and Mocko 2019). NLDAS-2 potential evapotranspiration data are computed using the modified Penman scheme (Mahrt and Ek 1984). Modified Penman PET uses temperature, wind speed, humidity, and solar radiation data to estimate PET, it is not estimated from temperature alone. NLDAS data are available back to 1979. Growing seasons 1980–2019 were evaluated here. The year 1979 was not included because computation of long-term drought indices during growing season 1979 would necessitate availability of 1978 data. NLDAS data were chosen for this study because of the dataset's length of record, continuity, and use in similar previous studies (e.g., Hobbins et al. 2016). Other datasets could have been used to complete this work. For example, GridMET assimilates NLDAS-2 data, and produces a 4-km CONUS product with daily precipitation and PET outputs (Abatzoglou 2011). Since CSPEIs are currently produced at county scale, the finer resolution was not necessary here.

b. Water balance computation

Meteorological conditions are monitored using NLDAS for corn, soybeans, and winter wheat throughout the model-parameterized growing season (MPGS). CSPEIs are computed for each day from planting to harvest. The MPGS is determined using a combination of agricultural data and meteorological data. MPGSs do not start until at least 50% of the crop has been planted according to National Agriculture Survey Statistics (NASS 2020a). These statistics do vary by year. If fields are too wet for planting (e.g., spring 2019), this will be reflected in NASS data. Since winter wheat is planted in the fall, the season starts at green-up date, which is also approximated with NASS data. For corn and soy, the MPGS may be delayed if freezing temperatures occur after the initial planting date. In such cases, the crop is "replanted" after the spring's final freeze.

The MPGS lasts until the crop planted reaches the number of growing degree days needed for harvest. Growing degree-day (GDD) requirements for each crop are listed in Table 1 (Allen et al. 1998). The formulas for computing growing

TABLE 1. Growing degree days needed (°C) to reach midseason conditions and harvest for corn, soybeans, and winter wheat.

Crop type	GDD mid	GDD end
Corn	630	1500
Soybeans	390	1060
Winter wheat	280	1140

TABLE 2. Crop coefficients for corn, soybeans, and winter wheat at the beginning, middle, and end of a growing season.

Crop type	K_c initial	K_c mid	K_c end
Corn	0.3	1.2	0.8
Soybeans	0.5	1.15	0.5
Winter wheat	0.2	1.15	0.3

degrees are given in Eqs. (1)–(3) (North Dakota Agricultural Weather Network Center 2020). In Eqs. (1)–(3), T_{max}, T_{min}, and T_{mean}, are the daily high, low, and mean temperature, respectively:

$$\text{for } T_{\text{mean}(x)} < 10: \ \text{GDD}_x = \ \text{GDD}_{x-1}, \tag{1}$$

$$\text{for } T_{\text{mean}(x)} > 10, \ T_{\text{max}(x)} < 30: \text{GDD}_x = \ \text{GDD}_{x-1} + \frac{T_{\text{max}(x)} + \ T_{\text{min}(x)}}{2} - 10, \tag{2}$$

$$\text{for } T_{\text{mean}(x)} > 10, \ T_{\text{max}(x)} > \ 30: \text{GDD}_x = \ \text{GDD}_{x-1} + \frac{30 \ + \ T_{\text{min}(x)}}{2} - 10. \tag{3}$$

Traditionally SPEIs are computed by standardizing precipitation accumulation minus potential evapotranspiration accumulation as in Eq. (4). Balance = aggregated water balance, P = precipitation accumulation, and PET = potential evapotranspiration accumulation from days 1:n:

$$\text{for } x = 1:n: \ \text{Balance}_x = \text{Balance}_{x-1} + \ P_x - \text{PET}_x. \tag{4}$$

In this study, a crop-specific water balance is determined using Eq. (5); P is accumulated precipitation, and ET_r is the reference ET for the crop. ET_r is computed based on crop coefficients (K_c) using Eq. (6):

$$\text{for } x = 1:n : \text{CSbalance}_x = \ \text{CSbalance}_{x-1} \ + \ P_{(x)} - \ \text{ETr}_{(x)}, \tag{5}$$

$$\text{ETr}_x = \ \text{PET}_x \times K_{c_x}.$$

Crop coefficients (K_c) for corn, soybeans, and winter wheat are provided in Table 2. The K_c initial, K_c mid, and K_c end indicate crop coefficient at the start, middle, and end of the growing cycle. Derivations for crop coefficients provided are available in Jensen and Allen (2016). Crop coefficients are interpolated between beginning, middle, and end season stages as the season progresses based on GDD. The crop coefficient interpolation scheme selected comes from the AgriMet Weather Station Network (USBR 2020). No irrigation parameterization is used in this water balance computation. This is worth noting particularly for crops in the western United States where irrigation is common practice.

To best make sense of the data, an analysis is presented detailing the climatology of crop-specific water balance ($P - \text{ET}_r$) over 1980–2019 MPGSs. We computed the mean and standard deviation of $P - \text{ET}_r$ for each county with sufficient data. For a county to be included in this analysis, there must be at least 20 years from 1980 to 2019 where 1) yield data are available and 2) enough growing degree days accumulated between the last and first freeze for a successful harvest to be parameterized.

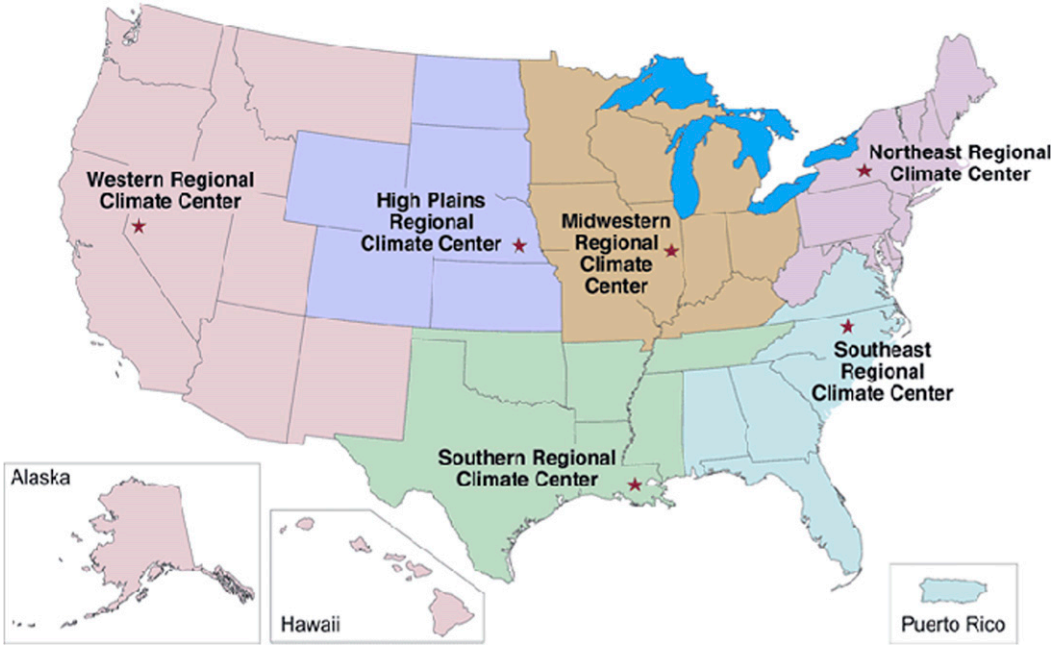

FIG. 1. United States climate regions as defined by the National Oceanic and Atmospheric Administration.

c. *Standardization*

Next, a CSPEI is computed for each day of the MPGS for each crop every year from 1980 to 2019 using the Beguería et al. (2014) procedure, which fits data to a log-logistic distribution, which is then adjusted using L-moments. A standardization process is necessary for maximum utility as a drought indicator since the U.S. Drought Monitor is designed using a percentile ranking classification system (Lawrimore et al. 2002).

SPI, EDDI, and SPEI all use different standardization processes. SPI and SPEI values are derived by fitting existing data to a curve. These curves follow gamma distributions in the case of the SPI and log-logistical distributions in the case of the SPEI. In both cases, the values used are those indicating how many standard deviations above or below the mean a given accumulation value would be if the cumulative density function fit to the dataset were normally distributed. Curve fitting is not used to derive EDDI values. EDDI values are standard deviation estimates based on weighted percentile values.

d. *Comparison to yields*

Corn, soybean, and winter wheat SPEIs were correlated to respective county-level crop yield data from USDA (NASS 2020a). We assessed the effectiveness of CSPEIs, and traditional indicators, in two ways: 1) What is the correlation between CSPEI and yields? 2) How widespread are statistically significant results within each NOAA NCEI Climate Region (NCEI 2020; Fig. 1)?

Yields of corn, soybeans, and winter wheat have all experienced increases between 1980 and 2019 due primarily to advances in crop genetics (Smith and Kurtz 2015). Yields were detrended using either a first- or second-order polynomial fit.

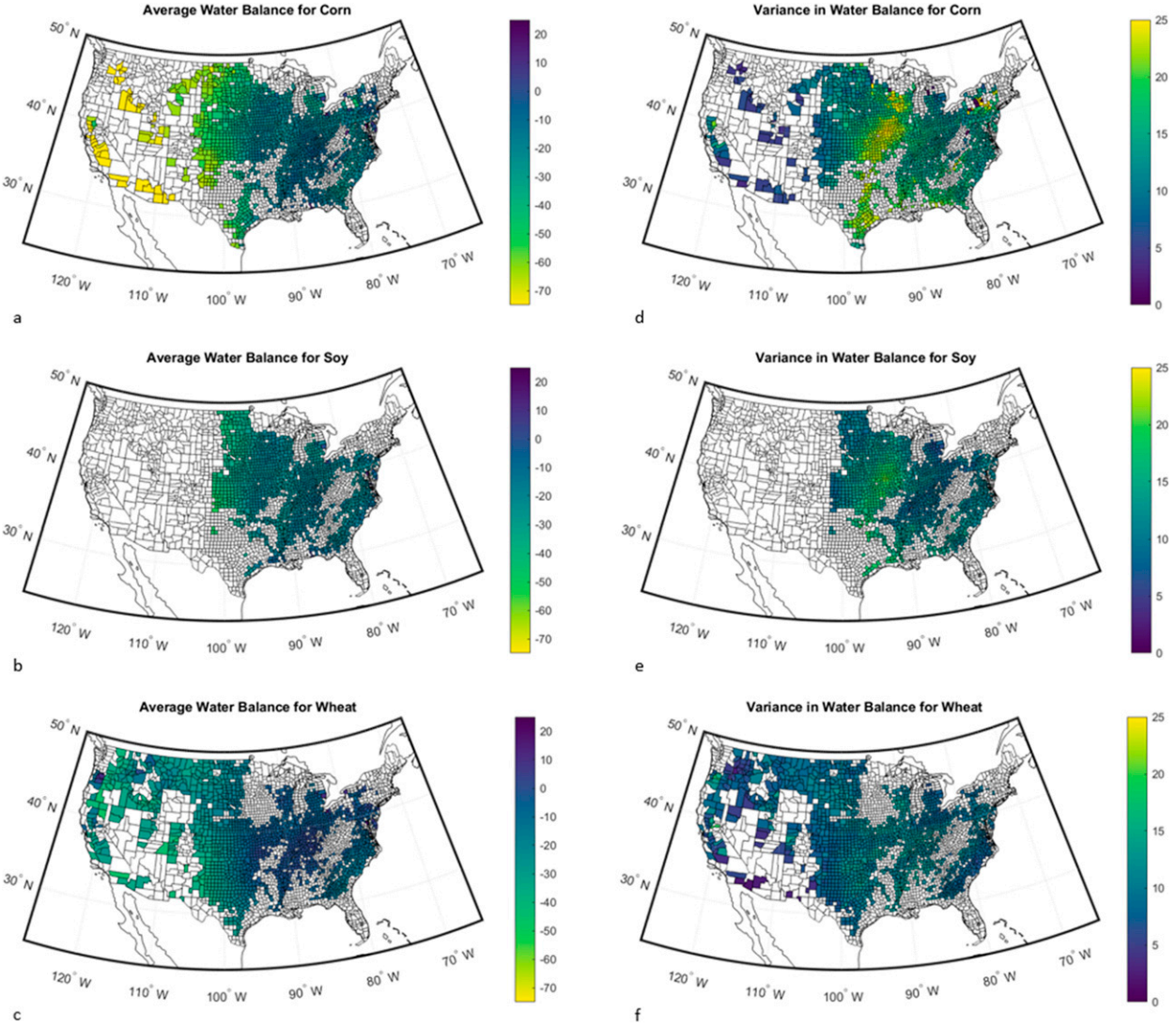

FIG. 2. (a)–(c) Modeled mean and (d)–(f) standard deviation of MPGS P − Ref ET (cm) for (top) corn, (middle) soybeans, and (bottom) winter wheat.

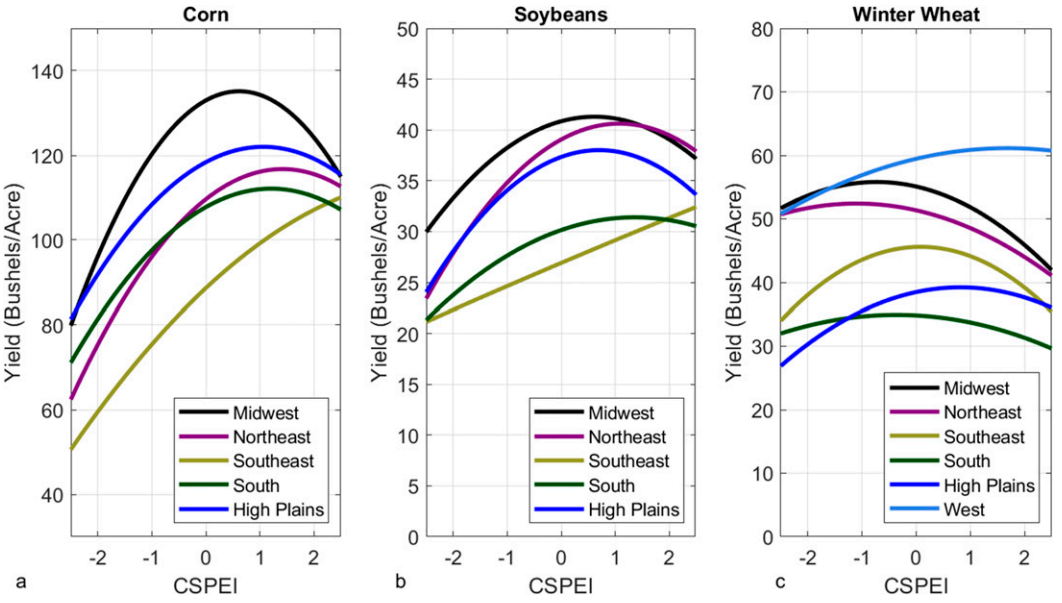

FIG. 3. Lines of best fit for CSPEIs vs crop yields by crop and region (colored lines).

The polynomial used for each county–crop combination was the one explaining the greatest amount of variance in yields. From here on out, all usage of the word "yields" refers to the detrended dataset.

There are a number of reasons why yields may decline, including flooding. But for the purposes of this study, CSPEI is only being evaluated as a drought indicator. Therefore, correlations between indices and yields were only computed for

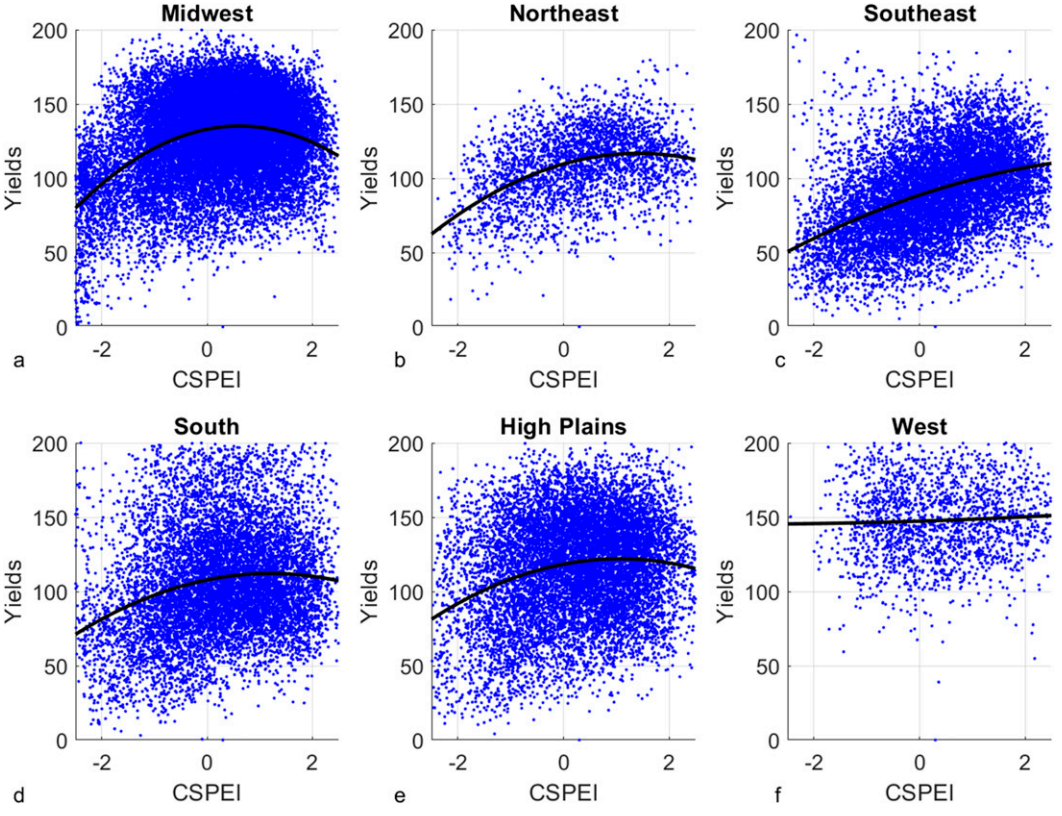

FIG. 4. Scatterplots of all CSPEI and yield pairs (blue dots) with lines of best fit (black) for corn for each climate region.

MPGSs where the drought index used was <0. The strength of the relationship between CSPEIs and the yields of the crops they represent is compared to several of the previously discussed drought indicators, namely, SPI, EDDI, and SPEI. These three indicators were chosen because they are ostensibly simpler forms of the CSPEI. Output from these indicators makes for a fair, direct comparison to CSPEI. The indicators were calculated using the same set of reanalysis data used to compute CSPEI. SPI, EDDI, and SPEI were computed using procedures outlined in McKee et al. (1993), Hobbins et al. (2016), and Beguería et al. (2014), respectively. SPI, EDDI, and SPEI are multiscalar, so several time scales were used (1, 3, 6, 9, and 12 months). Similar to CSPEI, correlations between SPI, EDDI, and SPEI were only evaluated for years where the index was <0. The years selected for correlation analysis were determined individually for each indicator, time scale, and accumulation period. For example, if 1 August 3-month SPI > 0 and 1 August 1-month SPI < 0 for a given year (e.g., 1995), 1995 indicator and yield data would be used in 1-month SPI correlation analysis, but not in 3-month analysis. Significance of correlation between drought indicator and yields was assessed using the t test in Eq. (7), where t is the t statistic, r is the correlation, df is the degrees of freedom ($n - 2$) when analyzing a linear correlation, and n is the number of years for which the tested drought indicator <0. The t statistic is compared to a critical value (CV), for $\alpha = 0.05$:

$$t = \frac{r \times \sqrt{\mathrm{df}}}{\sqrt{1 - r^2}}. \tag{7}$$

Additional analysis was conducted for counties in which 1) CSPEIs were significantly correlated with yields at 95% confidence and 2) CSPEIs were more closely correlated with yields than seasonal SPI, or 6-month SPIs ending between 15 August and 30 September for corn and soybeans, and between 1 June and 15 July for winter wheat. In these situations, climate and yield patterns in the years responsible for the largest differences between SPI and CSPEI were investigated.

3. Results

a. CSPEI climatology

MPGS water balance ($P - \mathrm{ET}_r$) increases across CONUS from west to east for all row crops tested (Figs. 2a–c). Average water balances over western CONUS were almost exclusively negative, in some cases by over 750 mm yr^{-1}, such as in the San Joaquin Valley, California (Figs. 2a,c).

MPGS water balance is negative more often for corn than soybeans or winter wheat. Corn produces more ET_r than

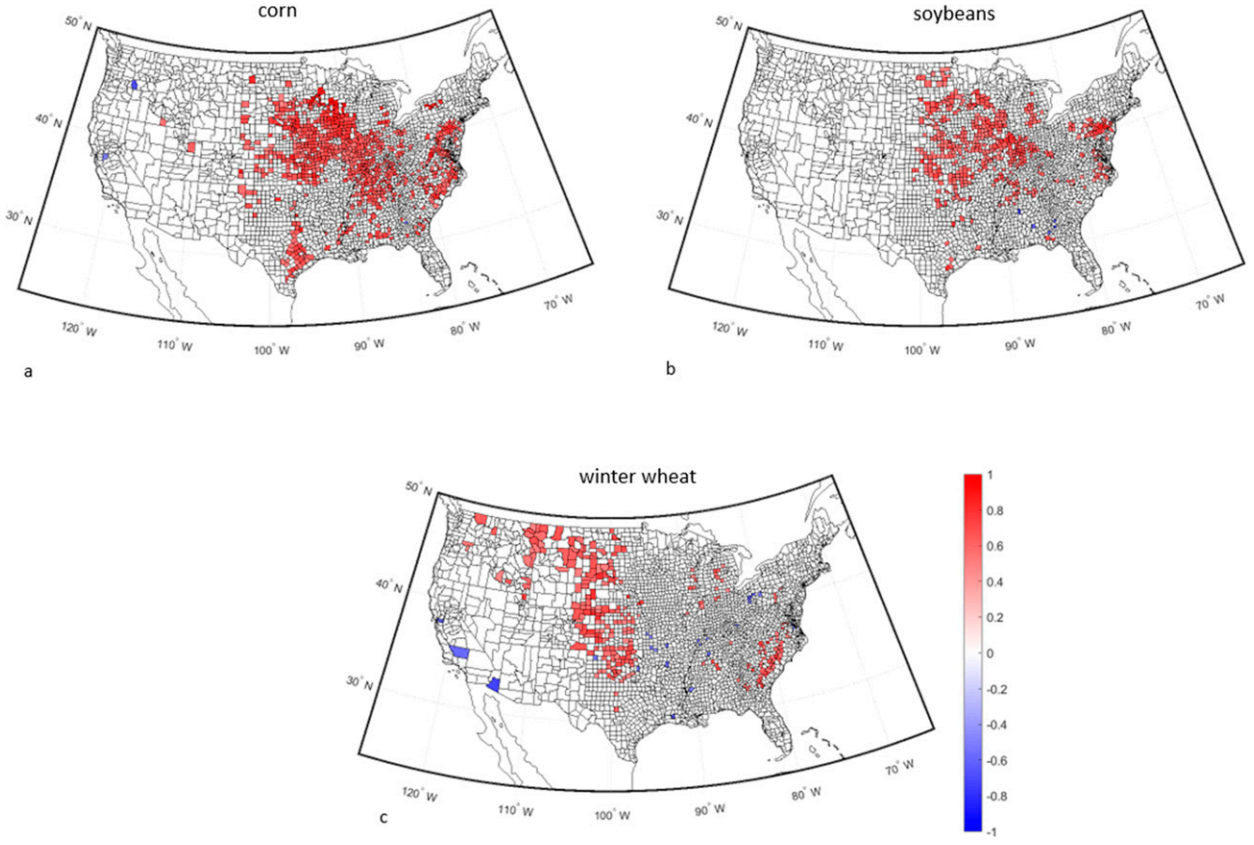

FIG. 5. Correlation between CSPEI and yields for (a) corn, (b) soybeans, and (c) winter wheat. Results masked for nonstatistically significant counties (95% confidence) ($r > 0.33$ for df = 19). Computed from years 1980–2018 for years with CSPEI < 0.

soybeans or winter wheat due to its longer growing season, and high mid-to-late season ET_r. Reference ET rates are higher for soybeans than winter wheat (Table 2). Water balance was not computed for soybeans west of 102°W, since there are so few planted west of the 102°W meridian. Winter wheat seasonal water balances had the lowest absolute values (Fig. 2f) due to its relatively short season from green-up to harvest. Still, for winter wheat, ET_r outpaces P in most years in the High Plains and the West.

The standard deviation in MPGS water balance averaged across all counties for corn, soybeans, and winter wheat were 156, 123, and 102 mm, respectively. Variance in seasonal water balance was highest over the central plains (Figs. 2d–f), a region known for high seasonal weather variability in both temperature and precipitation. Water balances may vary by over 250 mm from one year to the next. For example, western Missouri water balance in an average MPGS is near zero for corn. In 2012 this balance was between −600 and −900 mm, values akin to average conditions in central Arizona. Water balance in wet years, such as 1993 or 2015, was as high as +200 mm.

b. CSPEI versus yields

Yields are typically higher for corn, soybeans, and winter wheat when CSPEI is near zero than when CSPEI is much less than zero. Applying a second-order polynomial fit to all CSPEI and yield data for each region reveals that yields often decline similarly in both anomalously wet and anomalously dry conditions (Fig. 3). Water balance on the wet side of normal is most often preferred to dry. For corn and soybeans, optimal CSPEI values were between +0.5 and +1.5 for the Midwest, Northeast, South, and High Plains. For winter wheat, drier than normal conditions were shown to optimize yields in more climate regions. The highest yields occur when $-1.5 < \text{CSPEI} < 0$ for the Midwest, Northeast, and Southern climate regions. Extreme conditions, $|\text{CSPEI}| > 2$, were more harmful to yields when wet than dry in these regions (Fig. 3). $\text{CSPEI} > 0$ conditions were still favored to maximize yields in the Southeast, High Plains, and Western climate regions.

There is substantial scatter between CSPEI and yields. Figure 4 shows all the CSPEI–yield combinations for corn from 1980 to 2019. While the worst yields often occur during the driest of years, no CSPEI value should be considered a guarantee of above normal yields. This result is somewhat expected as agricultural damage is not a drought-only phenomenon. There are a number of weather-related events that can cause billion dollar agricultural disasters, to say nothing of unrelated threats (e.g., parasites). Such events include severe hail or windstorms, floods, and killing freezes (e.g., Smith 2020).

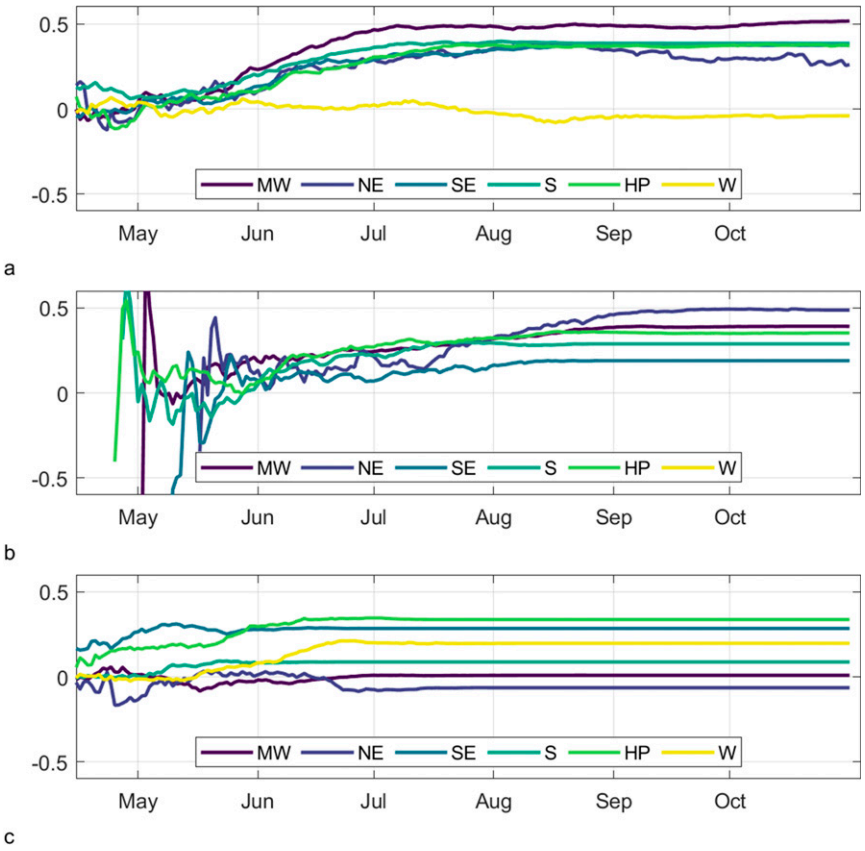

FIG. 6. Average county correlation between CSPEI and yields as a function of date for (a) corn, (b) soybeans, and (c) winter wheat.

Correlations were calculated between CSPEIs and end-of-season yields at a county level for all row crop–county combinations providing NASS yield data (Fig. 5). Since the goal is to test the impact of drought on yields, and not flooding or pluvial conditions, correlation was only computed for years in which MPGS CSPEI < 0. The correlation is statistically significant at 95% confidence for 42%, 31%, and 14% of eligible counties for corn, soybeans, and winter wheat, respectively. Statistical significance indicates correlations of 0.33 or greater, though the exact threshold changes as a function of number of years CSPEI < 0, and number of years with available crop yield data.

Correlations between CSPEI and yield were significant for corn over states where corn production is the highest, such as Iowa and Illinois (NASS 2020a). Scattered statistically significant correlations are found though the South and Southeast climate regions. Correlation between CSPEI and yields was significant across much of the Midwest for soybeans as well.

Winter wheat yield was strongly related to water balance through much of the High Plains including western Kansas, eastern Colorado, western South Dakota, and Montana. While only 14% of counties had a significant relationship, it was significant through the portion of CONUS with the highest winter wheat production, or the "wheat belt."

Very few counties exhibited a significantly negative correlation between CSPEI and yields. Such counties can be found in California and scattered through the Midwest and South. In the case of California, winter wheat is mostly irrigated, and irrigation is not considered in CSPEI computation. Figure 3 shows that average yields decline from CSPEI $= -1$ to CSPEI $= 0$ for both the Midwest and Southern climate regions, so it is not surprising that some counties have a significantly negative correlation between CSPEI and yields for years with CSPEI < 0.

Correlation between CSPEI and yields increases for the first two thirds of the growing season, and then becomes steady (Fig. 6). In the Midwest, the correlation between CSPEI and yield actually peaks in mid–July, and then decreases. This suggests a below normal water balance is less consequential to yields in the final third of the growing season for the Midwest.

The worst yield years often occur when CSPEI values are low (Fig. 7). Over 80% of yield values below the 5th percentile occur in years in which CSPEI < 0. This is true regardless of region. In the Midwest, 60% of <5th percentile corn yields occurred when CSPEI < -1. The drought of 2012 has a large impact on this result. Results are similar for soybeans, with over 75% of yield years $<$ 5th percentile occurring with CSPEI < 0. Results for winter wheat were different, with the worst yield years actually occurring when CSPEI > 0. For the Northeast, 65% of <5th percentile yield years occurred when CSPEI > 1. This may be because the Northeast climate region is an energy-limited region. Moisture is more abundant than warmth and sunshine, so wetter than normal years hurt winter wheat production more than help.

c. *CSPEI versus traditional indicators*

CSPEIs correlate more closely with crop yields in drier than normal years than most indicators in most regions. Figures 8–10 show correlation between CSPEI and yields for years in which CSPEI < 0, and correlation between traditional drought indicators and yields at various time scales and

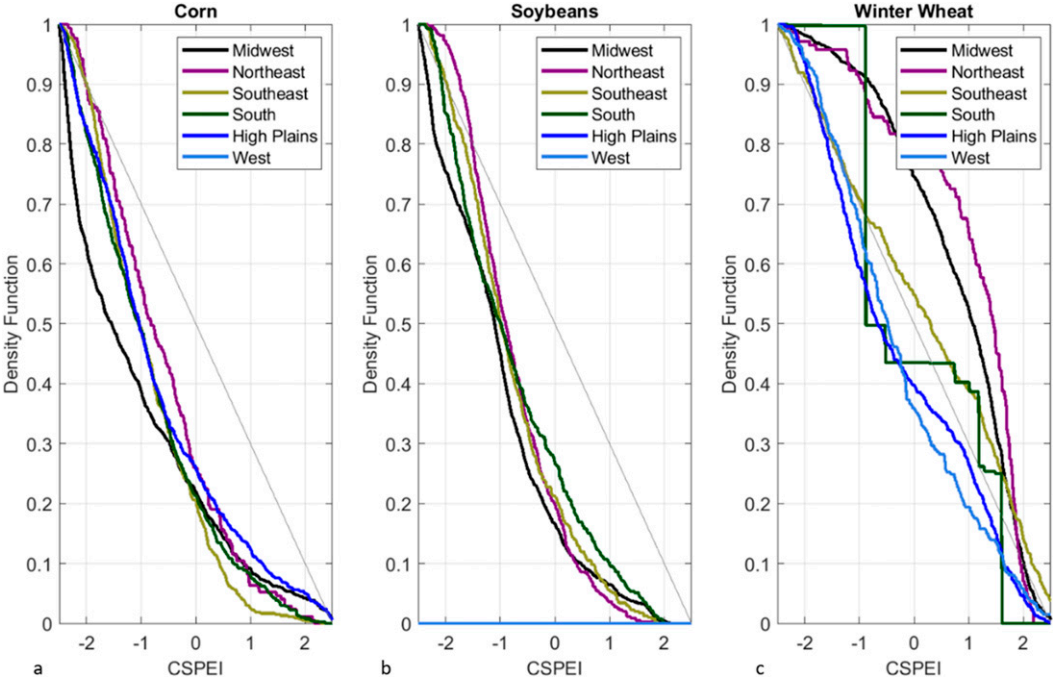

FIG. 7. Fraction of <5th percentile yield years among all counties in which CSPEI value was below value X for (a) corn, (b) soybeans, and (c) winter wheat. Computed for all climate regions (colored lines) from growing seasons 1980–2018.

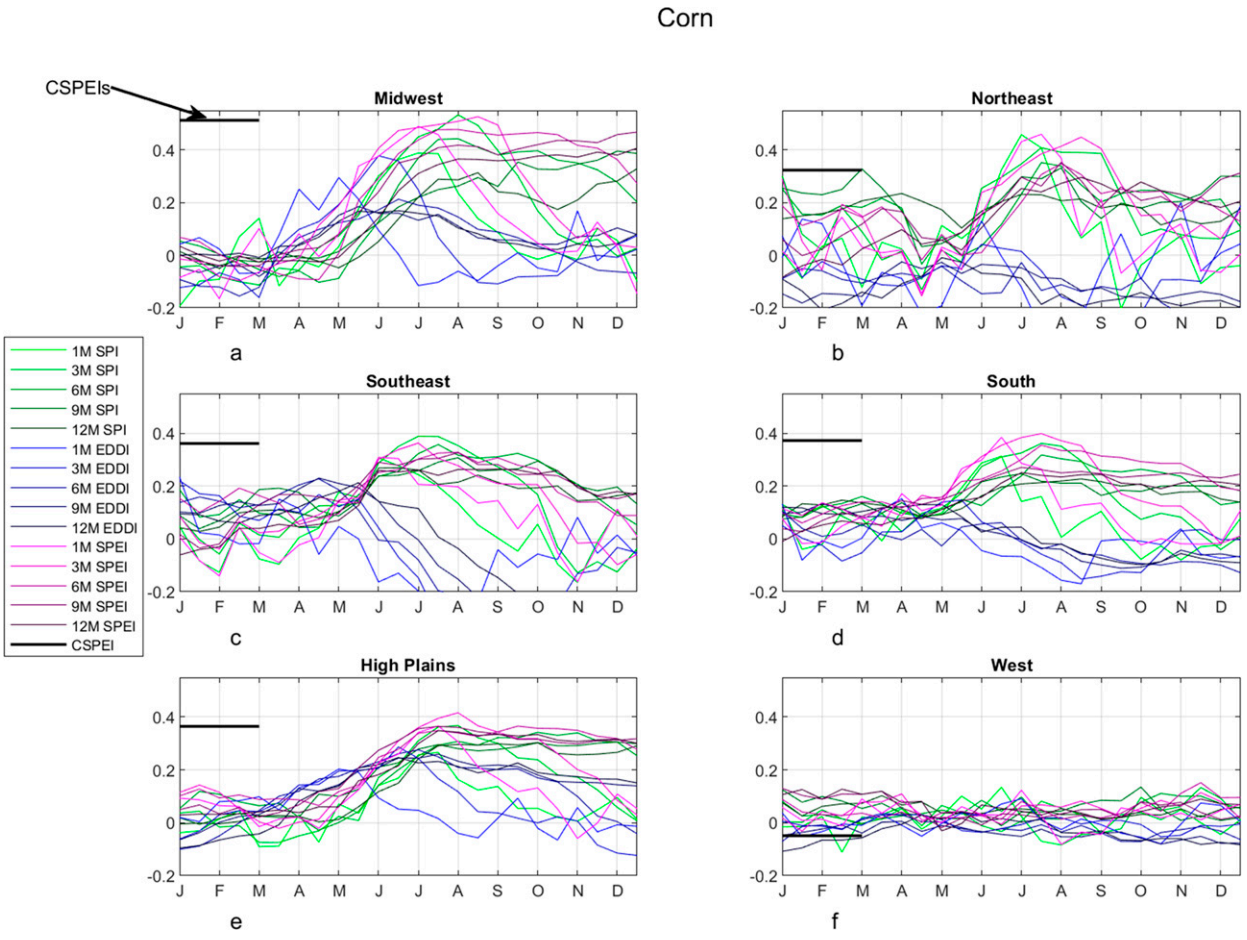

FIG. 8. Average correlation between drought indicators and yields by region for corn: (a) Midwest, (b) Northeast, (c) Southeast, (d) South, (e) High Plains, and (f) West. Region average correlation between growing season CSPEIs and yields shown using tick marks on left of each panel. Colored lines show region average correlations between traditional drought indicators for aggregation periods ending at time of year shown on the x axis, and crop yields. Green = SPI, blue = EDDI, purple = SPEI. Indices shaded by aggregation length (darker = longer, lighter = shorter). Correlations only computed for years in which drought index < 0.

seasons for years in which index < 0. These figures provide strong evidence that growing season weather conditions, particularly precipitation, are important for estimating row crop yields. CSPEIs are more closely correlated with yields than nearly all traditional indicators tested for the Midwest, Northeast, Southeast, South, and High Plains for corn and soybeans. When compared with 360 traditional indicators, CSPEI was one of the top three highest correlated indices for a number of crop–region combinations. Examples include corn in the Midwest, soybeans in the Northeast, corn and winter wheat in the Southeast, and corn in the South. However, at least one traditional indicator was more strongly correlated to yields for all crop–region combinations.

The traditional drought indicators most strongly correlated to yields were SPIs or SPEIs with short aggregation periods in the middle of the growing season. The drought indices most closely correlated with yields for corn and soybeans were SPI or SPEI of 1–3 months in length ending between July and October. Water balance over the full growing season is therefore less indicative of yields than water balance over the mid-growing season. Crop type impacted which drought indicator was best, likely due to differences in crop seasonal cycle. Winter wheat green-up occurs earlier than corn or soybean planting season. Soybeans are typically planted after corn. Correlation between drought indicators and yields peaked earliest for winter wheat and latest for soybeans.

CSPEIs compared most closely to 6-month duration drought indicators. This is the aggregation period on average most similar to CSPEI (Fig. 11). CSPEIs were more closely correlated with yields in dry years than any 6-month indicator for corn in the Midwest, Southeast, South, and High Plains, and for soybeans in the Northeast, and for winter wheat in the High Plains. In these cases, the closest traditional indicators to equal correlation strength were SPI or SPEI ending in September or October. CSPEIs did not explain more variance in yields than 6-month SPIs or SPEIs for soybeans in the Midwest, Southeast, or South. This may be due to the long planting season for soybeans in southern regions. One could argue

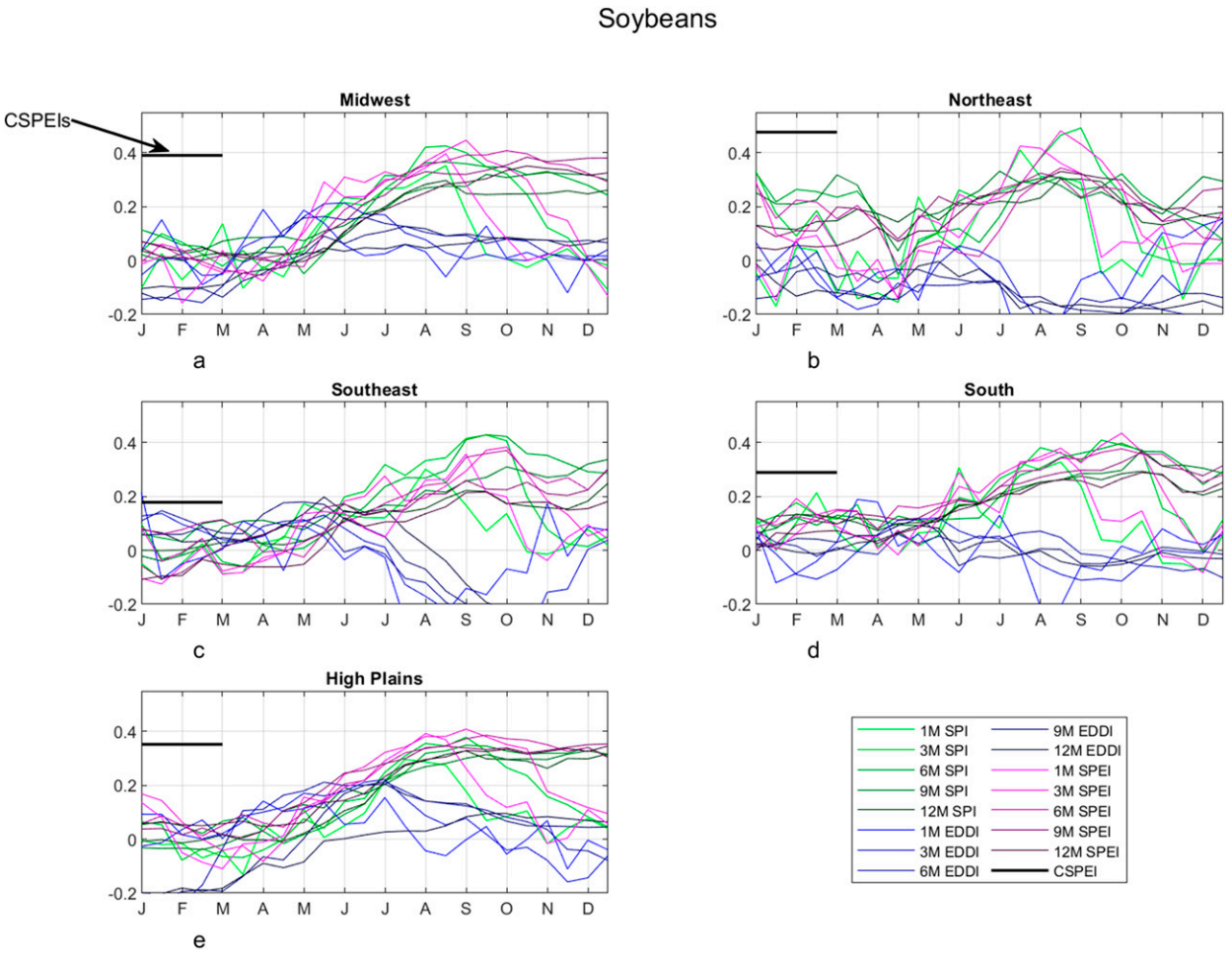

FIG. 9. Average correlation between drought indicators and yields by region for soybeans: (a) Midwest, (b) Northeast, (c) Southeast, (d) South, (e) High Plains. Region average correlation between growing season CSPEIs and yields shown using tick marks on left of each panel. Colored lines show region average correlations between traditional drought indicators for aggregation periods ending at time of year shown on the *x* axis, and crop yields. Green = SPI, blue = EDDI, purple = SPEI. Indices shaded by aggregation length (darker = longer, lighter = shorter). Correlations only computed for years in which drought index < 0.

that two CSPEIs are necessary for soybeans in the South and Southeast climate regions, as planting date is bimodal (NASS 2020a). Soybean planting peaks in April/May, and again in July/August.

Nationwide, CSPEIs performed more poorly for winter wheat than corn or soybeans. This is evident comparing CSPEIs to other drought indicators (Figs. 8–11). For example, 6-month SPEIs during the warm season are significantly more correlated to winter wheat yields in dry years than CSPEIs in the Midwest (Fig. 11). The 6-month EDDIs are significantly more correlated to winter wheat yields than CSPEIs in the Northeast. CSPEIs are poorly correlated to winter wheat yields in general throughout the Western climate region.

d. Notable CSPEI successes

There are areas over CONUS for which CSPEI was significantly correlated with yields, and more closely correlated with yields than growing season SPI for corn, soybeans, and winter wheat. Figure 12 shows the counties in which CSPEI is both significantly correlated to yields, and more closely correlated than the highest correlated 6-month SPI ending between 15 August and 30 September for corn and soybeans, and between 1 June and 15 July for winter wheat.

For winter wheat, CSPEIs are more correlated to yields than 6-month SPIs over the majority of the western High Plains region. For these counties, the best traditional drought metrics were 9-month SPIs ending in June, which include fall and early winter precipitation, and 30-day EDDI in June. The CSPEI does not include fall precipitation but is more closely correlated to yields than 6-month SPI because mid-to-late season evaporative demand impacts yields.

Only a small fraction of CONUS counties sees a stronger correlation between soy CSPEI and soybean yields than 6-month growing season SPIs. This may be due to the long, flexible planting season for soybeans. The exact growing season is

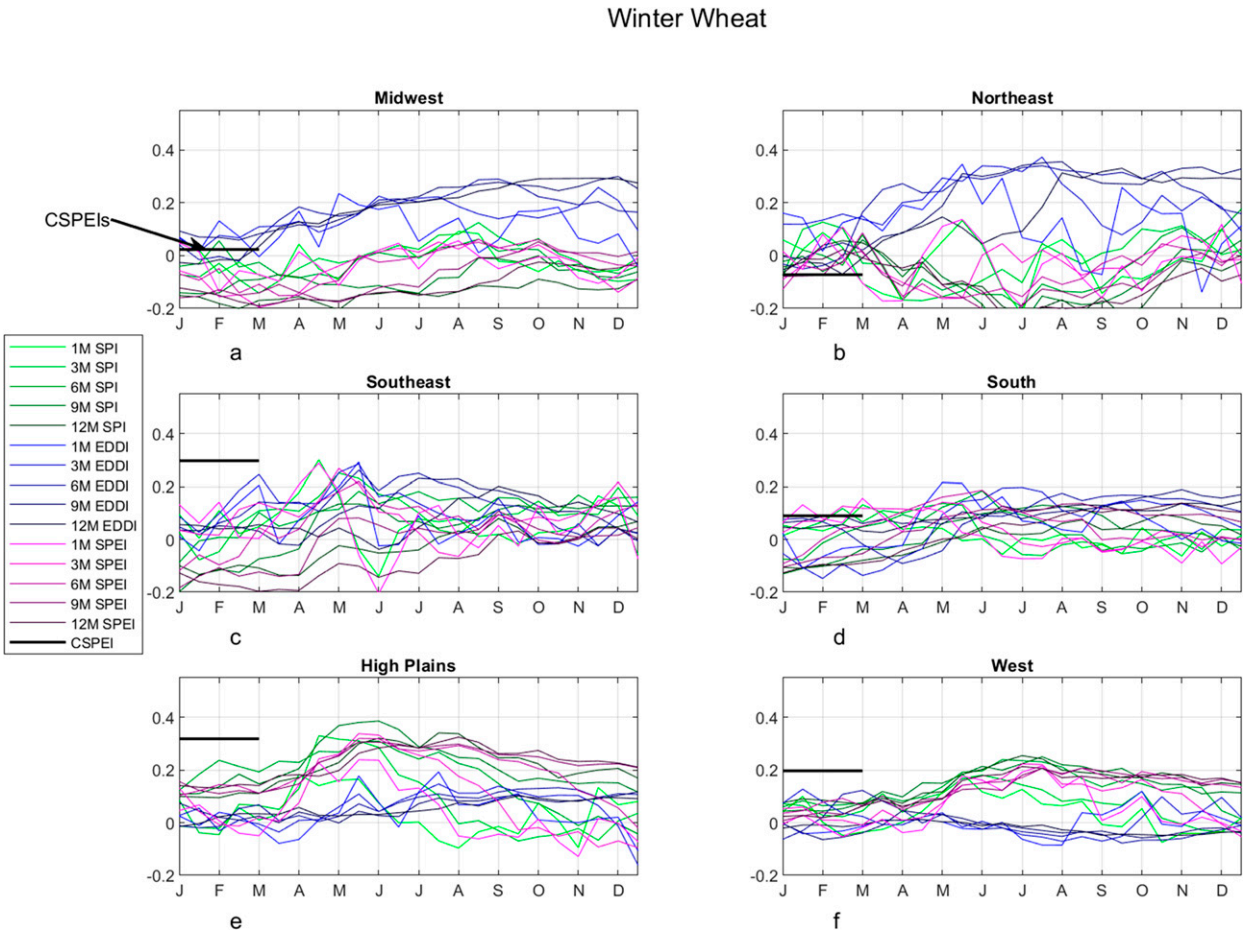

FIG. 10. Average correlation between drought indicators and yields by region for winter wheat: (a) Midwest, (b) Northeast, (c) Southeast, (d) South, (e) High Plains, (f) West. Region average correlation between growing season CSPEIs and yields shown using tick marks on left of each panel. Colored lines show region average correlations between traditional drought indicators for aggregation periods ending at time of year shown on the x axis, and crop yields. Green = SPI, blue = EDDI, purple = SPEI. Indices shaded by aggregation length (darker = longer, lighter = shorter). Correlations only computed for years in which drought index < 0.

more difficult to parameterize for soybeans, making CSPEIs less effective.

Corn CSPEIs are more closely correlated to yields in dry years than 6-month SPIs for portions of the High Plains, Midwest, South, and Southeast regions (Fig. 12a). There is a downward trend in CSPEI driven by increased PET in recent warm years. This trend is not detected in SPI. As a result, some of the years with the greatest difference between SPI and CSPEI are recent, hot summers. Figure 13 shows the difference between CSPEI and growing season SPI for counties highlighted in Fig. 12a. We see here the relationship between SPI and CSPEI is changing as summers warm. Detecting this trend leads to better correlation with yields in some cases. For instance, corn CSPEIs were significantly lower than SPIs in 2012 for counties highlighted in Fig. 12a in the Midwest, High Plains, and Southeast at 99% confidence. Yields were also lower in these counties than the average Midwest County by an average of 10 bushels per acre. This indicates even if SPIs are not extremely poor, corn yields may still be strongly suppressed by summers with anomalously high reference ET. Similar examples can be seen in the Southern climate region in 2009 and 2011, which were both hot summers. CSPEIs were lower than SPIs in the south in these low yield years and were more closely correlated to yields as a result.

The greatest difference between CSPEI and SPI occurred in the Midwest for corn in 2014. This was a cool, wet summer with above normal yields. NLDAS-2 still indicated higher than normal PET, leading to above normal ET_r in CSPEIs. For most counties, SPIs this year were positive, so 2014 was not included in correlation analysis of dry years. On the other hand, the majority of CSPEIs were negative, and decreased the correlation between CSPEIs and yields. This merits further investigation as well.

There are critical stages of growth for corn, such as silking and tasseling, that may only last a few days (Çakir 2004). Extreme hot and dry weather may have a large impact on yields during such phases. This study is performed at too coarse a resolution to capture such effects. Future investigations of the

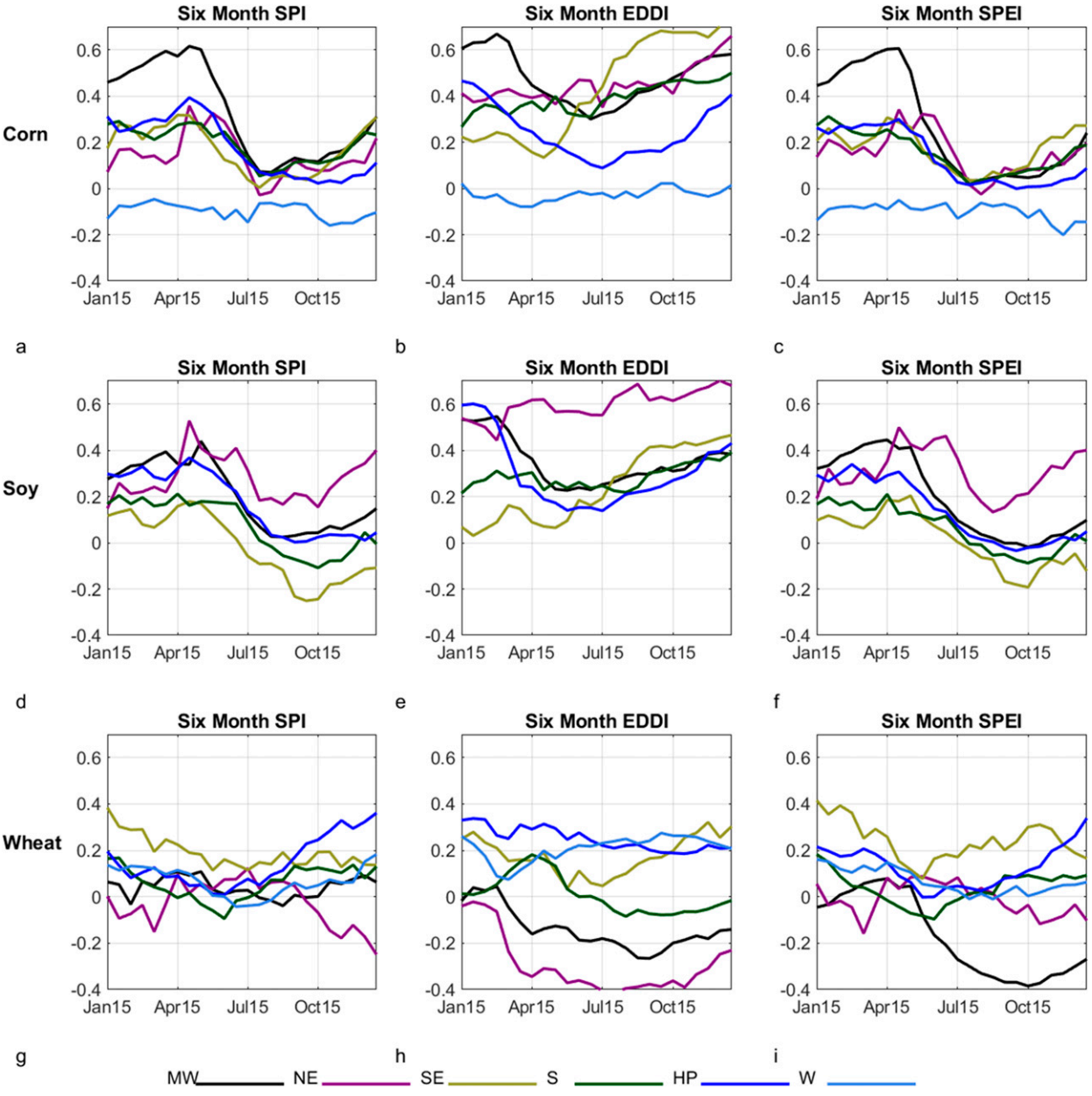

FIG. 11. [Correlation between MPGS CSPEI and (a)–(c) corn, (d)–(f) soybeans, and (g)–(i) winter wheat yields for years in which CSPEI < 0] − [Correlation between 6-month (left) SPI, (center) EDDI, (right) SPEI and corn, soybeans, and winter wheat yields for years in which index < 0] for MW = Midwest (black), NE = Northeast (purple), SE = Southeast (gold), S = South (green), HP = High Plains (blue), and W = West (cyan).

relationship between climate variables and crop yields should seek to understand these connections more closely.

4. Discussion

Due to the multifaceted and multiscalar nature of drought, assessing severity is not a straightforward endeavor. We developed a group of indices designed to appraise severity of drought over specific row crops (corn, soybeans, winter wheat) called crop-specific standardized precipitation–evapotranspiration indices (CSPEIs) to add clarity to the agricultural drought monitoring process. CSPEIs have the following helpful properties: they are data driven, available in near–real time, combine meteorological and phenological data, and in many cases correlate significantly with crop yields.

Results indicate that optimal yields often occur when growing season CSPEIs are greater than zero. For most crops and climate regions yields are highest when $0 < \text{CSPEI} < 1$.

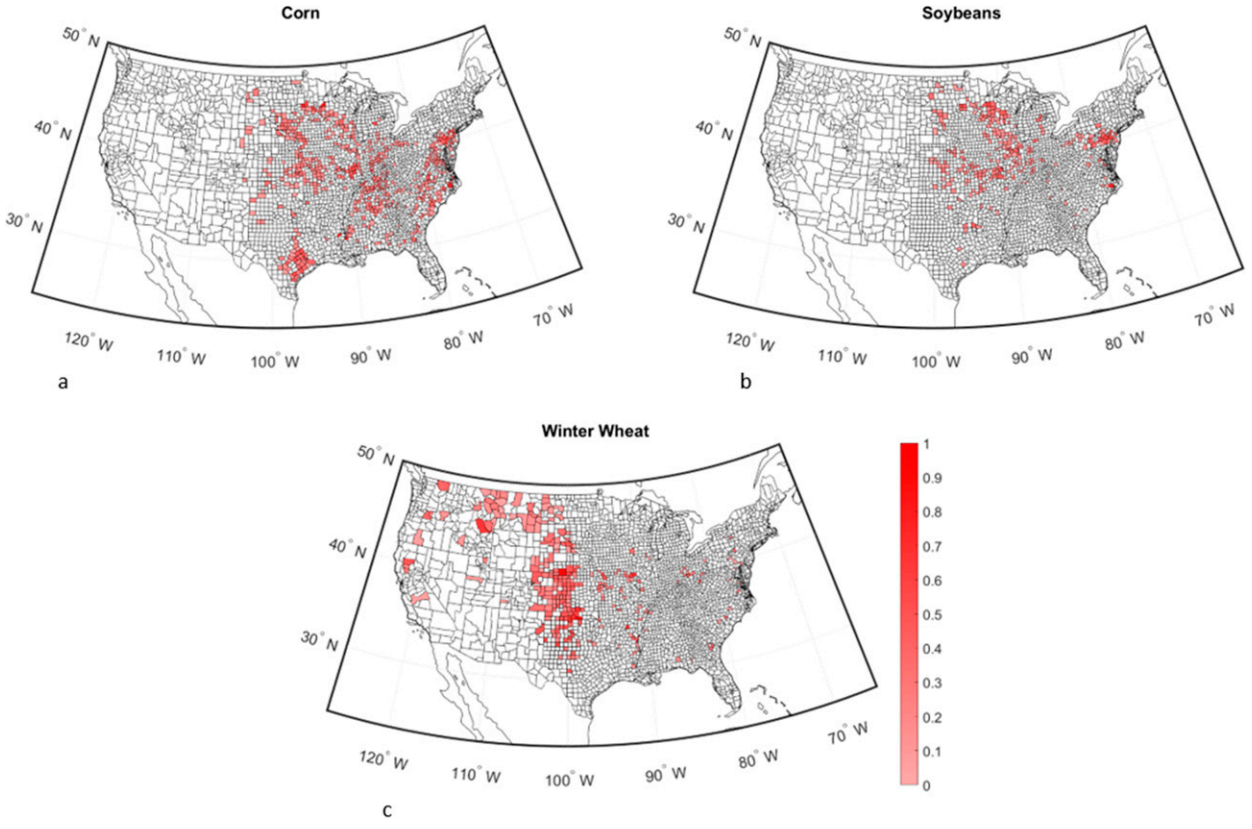

FIG. 12. Difference in correlation between CSPEI and yields and 6-month SPI and yields. Counties in red are 1) significantly correlated with crop yields for years in which CSPEI < 0 and 2) more closely correlated to yields than the highest correlated 6-month SPI ending between 15 August and 30 September. Deeper red shadings indicate a greater difference between CSPEI and SPI. All other counties shown in white. Results shown for (a) corn, (b) soybeans, and (c) winter wheat.

Examples include the Midwest, Northeast, South, and High Plains for corn; Midwest, South, and High Plains for soybeans; and High Plains for winter wheat. Yields decline at both dry and wet extremes. The majority of bottom 5th percentile yields occur in years where CSPEIs are low. There are some exceptions. The worst winter wheat yield years occurred primarily during wet extremes for the Midwest, Northeast, and South.

CSPEIs are positively correlated with yields for the largest field crops over CONUS: corn, soybeans, and winter wheat, in drier than normal years. Statistical significance is scattered in some cases (e.g., soybeans in the Midwest), and nonexistent in others (e.g., winter wheat in eastern regions). But generally, CSPEIs do correlate significantly with yields for crop–location combinations where the crop is considered a "major crop" by USDA. Notable examples include the Midwest and South for corn, the Midwest for soybeans, and the High Plains for winter wheat. Moisture is often plentiful over eastern CONUS, and plant growth is therefore fundamentally limited by amount of solar energy received. In the dry west, crop growth is limited by moisture. Regions in between, such as the central plains, are transitional zones between energy and moisture-limited climates (Budyko 1974; Seager et al. 2018). Both a crop water balance model, and an actual crop, should be sensitive to weather variations in transitional regions. Previous studies suggest this boundary extends from Texas northward through Oklahoma, Kansas, and Nebraska (e.g., Koster et al. 2004, 2011; Wei and Dirmeyer 2012). One might expect these regions to be especially sensitive to seasonal moisture anomalies. Correlations between CSPEI and yields were higher over central CONUS than the moisture-limited west or energy-limited east.

Assessment of existing indicators: SPI, EDDI, SPEI, over varying seasons and aggregation periods indicates growing season precipitation is significantly indicative of yields. The addition of PET, or ET_r, to index computation usually resulted in small changes to correlation with yield. SPIs, SPEIs, and CSPEIs all performed similarly over the growing season. This is a curious result and merits further study. In theory, higher PET or ET_r should trigger plant stress, and therefore impact yields (e.g., Meyer et al. 1993a,b; Moorhead et al. 2013). Results may be different with a different reanalysis dataset. Even so, CSPEIs are marginally more closely correlated with yields than warm season 6-month SPIs and SPEIs in the Midwest, High Plains, Southeast, and South for corn, and in the northeast for soybeans.

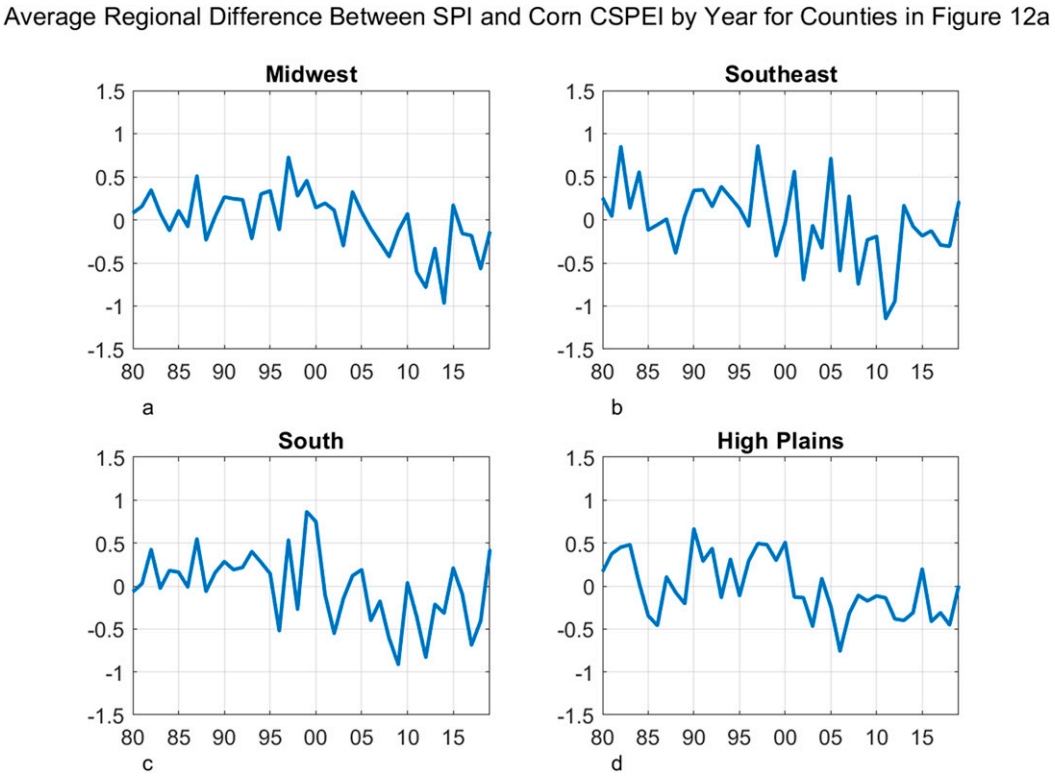

FIG. 13. Average regional difference between corn CSPEI and 6-month SPI ending between 15 August and 30 September most highly correlated to yields as a function of time. Computed for counties in which 1) CSPEI more closely correlated to yields than SPI in years where drought index < 0, and 2) CSPEI significantly correlated to yields at 95% confidence for years in which CSPEI < 0. Organized by region (a) Midwest, (b) Southeast, (c) South, (d) High Plains.

Typically, either a 1- or 3-month SPI or SPEI with an aggregation period ending between July and September was the tested index correlated most strongly to yields. In the cases of corn and soybeans, the highest performing traditional indicators were those that captured the middle period of the crop's growth cycle. This may indicate one need only monitor the middle of corn or soybean growth cycles to best predict yields from weather data.

CSPEIs presented here oversimplify true crop water balance in several ways. First, antecedent soil moisture was not considered. This can create inaccuracies in monitoring crop conditions in anomalously wet or dry winters. In 2019, for instance, fields were flooded for weeks across much of the American heartland (Irwin and Hubbs 2019). On the dry side, winter wheat producers may face difficulties long before spring green up if soils are dry during fall planting season. This could possibly be remedied by assigning a start-of-season CSPEI value based on soil moisture output [e.g., Variable Infiltration Capacity (VIC) model (Yuan et al. 2019)]. Second, growing crops over much of the western United States is only sustainable through irrigation, which is not considered in the computation of CSPEIs. Winter snowpack, and summer temperatures may be better indicators of yield for runoff-fed irrigation zones such as California's San Joaquin Valley.

CSPEIs are both significantly correlated with yields, and more closely correlated with yields than SPIs for drier than normal years in portions of the High Plains region for winter wheat, and portions of the High Plains, Midwest, South, and Southeast for corn. Differences between the two metrics were largest during recent hot, dry summers such as 2011 in the South, and 2012 for the High Plains and Midwest. Differences between CSPEI and SPI are likely to become more apparent in a warmer climate.

Nowhere near all available drought indicators were used in this study; there are hundreds, many with flexible data aggregation periods (Svoboda and Fuchs 2016). As such, correlating drought indicators to yields is a process that could be repeated endlessly. While crop-specific indices do produce an advantage over precipitation and evapotranspiration-based metrics of similar aggregation length, indices that remotely sense vegetative health, such as the vegetative health index (Bento et al. 2018), evaporative stress index (Otkin et al. 2013), and vegetation drought response index (Brown et al. 2008) may perform even better. However, these indicators have not been computed over as many years of record, and therefore do not offer as many years of data for testing.

The late Dr. Kelly Redmond once said, "In essence, as with rainbows, each person experiences their own drought." While

it remains impossible to objectively monitor every producer's individual experience with drought, CSPEIs do add clarity to the agricultural drought monitoring process.

Acknowledgments. The authors thank two anonymous reviewers for helpful suggestions that led to an improved manuscript. This research was funded by the National Oceanic and Atmospheric Administration's (NOAA) National Integrated Drought Information System (NIDIS), Awards NA19OAR4320073 and NA18OAR4310253B.

Data availability statement. Forcing data used to construct CSPEIs for this study were courtesy of the National Aeronautics and Space Association North American Land Data Assimilation Systems (NLDAS) (Rui and Mocko 2019). Post-processed CSPEI data are available from corresponding author upon request.

REFERENCES

Abatzoglou, J. T. 2011: Development of gridded surface meteorological data for ecological applications and modelling. *Int. J. Climatol.*, **33**, 121–131, https://doi.org/10.1002/joc.3413.

——, D. J. McEvoy, and K. T. Redmond, 2017: The West Wide Drought Tracker: Drought monitoring at fine spatial scales. *Bull. Amer. Meteor. Soc.*, **98**, 1815–1820, https://doi.org/10.1175/BAMS-D-16-0193.1.

Al-Kaisi, M. M., and Coauthors, 2013: Drought impact on crop production and the soil environment: 2012 experiences from Iowa. *J. Soil Water Conserv.*, **68**, 19A–24A, https://doi.org/10.2489/jswc.68.1.19A.

Allen, R. G., L. S. Pereira, D. Raes, and M. Smith, 1998: Crop evapotranspiration: Guidelines for computing crop water requirements. FAO Irrigation and Drainage Paper 56, 300 pp., www.fao.org/docrep/X0490E/X0490E00.htm.

Alley, W. M., 1984: The Palmer drought severity index: Limitations and assumptions. *J. Appl. Meteor. Climatol.*, **23**, 1100–1109, https://doi.org/10.1175/1520-0450(1984)023<1100:TPDSIL>2.0.CO;2.

——, 1985: The Palmer severity drought index as a measure of hydrologic drought. *J. Amer. Water Resour. Assoc.*, **21**, 105–114, https://doi.org/10.1111/j.1752-1688.1985.tb05357.x.

American Meteorological Society, 2020: Drought. Glossary of Meteorology, https://glossary.ametsoc.org/wiki/Drought.

Beguería, S., S. M. Vicente-Serrano, F. Reig, and B. Latorre, 2014: Standardized Precipitation Evapotranspiration Index (SPEI) revisited: Parameter fitting, evapotranspiration models, tools, datasets and drought monitoring. *Int. J. Climatol.*, **34**, 3001–3023, https://doi.org/10.1002/joc.3887.

Belal, A., H. R. El-Ramady, and E. S. Mohamed, 2014: Drought risk assessment using remote sensing and GIS techniques. *Arab. J. Geosci.*, **7**, 35–53, https://doi.org/10.1007/s12517-012-0707-2.

Benson, L. V., K. Petersen, and J. Stein, 2006: Anasazi (pre-Columbian Native American) migrations during the middle-12th and late-13th centuries—Were they drought induced? *Climatic Change*, **83**, 187–213, https://doi.org/10.1007/s10584-006-9065-y.

Bento, V. A., C. M. Gouveia, C. C. DaCamara, and I. F. Trigo, 2018: A climatological assessment of drought impact on Vegetation Health Index. *Agric. For. Meteor.*, **259**, 286–295, https://doi.org/10.1016/j.agrformet.2018.05.014.

Brown, J. F., B. D. Wardlow, T. Tadesse, M. J. Hayes, and B. C. Reed, 2008: The Vegetation Drought Response Index (Veg-DRI): A new integrated approach for monitoring drought stress in vegetation. *Geosci. Remote Sens.*, **45**, 16–46, https://doi.org/10.2747/1548-1603.45.1.16.

Budyko, M. I., 1974: *Climate and Life*. D. H. Miller, Ed., International Geophysics Series, Vol. **18**, Academic Press, 508 pp.

Çakir, R., 2004: Effect of water stress at different developmental stages on vegetative and reproductive growth of corn. *Field Crops Res.*, **89**, 1–16, https://doi.org/10.1016/j.fcr.2004.01.005.

Clayton, J. A., S. Quiring, T. Ochsner, M. Cosh, C. B. Baker, T. Ford, J. D. Bolten, and M. Woloszyn, 2019: Building a one-stop show for soil moisture information. *Eos*, **100**, https://doi.org/10.1029/2019EO123631.

Daly, C., M. Halbleib, J. I. Smith, W. P. Gibson, M. K. Doggett, G. H. Taylor, J. Curtis, and P. P. Pasteris, 2008: Physiographically sensitive mapping of climatological temperature and precipitation across the conterminous United States. *Int. J. Climatol.*, **28**, 2031–2064, https://doi.org/10.1002/joc.1688.

Emanuel, K., 2005: Increasing destructiveness of tropical cyclones over the past 30 years. *Nature*, **436**, 686–688, https://doi.org/10.1038/nature03906.

Entekhabi, D., and Coauthors, 2010: The Soil Moisture Active Passive (SMAP) mission. *Proc. IEEE*, **98**, 704–716, https://doi.org/10.1109/JPROC.2010.2043918.

Groisman, P. Ya., R. W. Knight, T. R. Karl, D. R. Easterling, B. Sun, and J. H. Lawrimore, 2004: Contemporary changes of the hydrological cycle over the contiguous United States: Trends derived from in situ observations. *J. Hydrometeor.*, **5**, 64–85, https://doi.org/10.1175/1525-7541(2004)005<0064:CCOTHC>2.0.CO;2.

Hobbins, M. T., A. Wood, D. J. McEvoy, J. L. Huntington, C. Morton, M. Anderson, and C. Hain, 2016: The evaporative demand drought index. Part I: Linking drought evolution to variations in evaporative demand. *J. Hydrometeor.*, **17**, 1745–1761, https://doi.org/10.1175/JHM-D-15-0121.1.

House of Representatives, 2018: Providing for consideration of the conference report to accompany the bill (H.R. 2) to provide for the reform and continuation of agricultural and other programs of the Department of Agriculture through fiscal year 2023, and for other purposes. H.R. Res. 1776, 115th Congress, https://www.congress.gov/bill/115th-congress/house-resolution/1176/all-info.

Irwin, S., and T. Hubbs, 2019: Late planting and projections of 2019 U.S. corn and soybean acreage. *Farmdoc daily*, No. (9):85, Department of Agricultural and Consumer Economics, University of Illinois at Urbana–Champaign, 7 pp., https://farmdocdaily.illinois.edu/2019/05/late-planting-and-projections-of-2019-u-s-corn-and-soybean-acreage.html.

Jensen, M. E., and R. G. Allen, Eds., 2016: Appendix B: Mean crop coefficients in subhumid climates. *Evaporation, Evapotranspiration, and Irrigation Water Requirements.* 2nd ed. American Society of Civil Engineers, 471–485.

Koster, R. D., and Coauthors, 2004: Regions of strong coupling between soil moisture and precipitation. *Science*, **305**, 1138–1140, https://doi.org/10.1126/science.1100217.

——, and Coauthors, 2011: The second phase of the global land–Atmosphere coupling experiment: Soil moisture contributions to subseasonal forecast skill. *J. Hydrometeor.*, **12**, 805–822, https://doi.org/10.1175/2011JHM1365.1.

Kwon, H. H., and U. Lall, 2016: A copula-based nonstationary frequency analysis for the 2012–2015 drought in California. *Water Resour. Res.*, **52**, 5662–5675, https://doi.org/10.1002/2016WR018959.

Lackstrom, K., A. Farris, D. Eckhardt, N. Doesken, H. Reges, J. Turner, K. H. Smith, and R. Ward, 2017: CoCoRaHS observers contribute to "condition monitoring" in the Carolinas: A new initiative addresses needs for drought impacts information. *Bull. Amer. Meteor. Soc.*, **98**, 2527–2531, https://doi.org/10.1175/BAMS-D-16-0306.1.

Lawrimore, J., R. R. Heim Jr., M. Svoboda, V. Swail, and P. J. Englehart, 2002: Beginning a new era of drought monitoring across North America. *Bull. Amer. Meteor. Soc.*, **83**, 1191–1192, https://doi.org/10.1175/1520-0477-83.8.1191.

Lesk, C., P. Rowhani, and N. Ramankutty, 2016: Influence of extreme weather disasters on global crop production. *Nature*, **529**, 84–87, https://doi.org/10.1038/nature16467.

Liu, Y., Y. Zhu, L. L. V. P. Singh, X. Yang, and F. Yuan, 2017: A multiscalar Palmer drought severity index. *Geophys. Res. Lett.*, **44**, 6850–6858, https://doi.org/10.1002/2017GL073871.

Mahrt, L., and M. Ek, 1984: The influence of atmospheric stability on potential evaporation. *J. Climate Appl. Meteor.*, **23**, 222–234, https://doi.org/10.1175/1520-0450(1984)023<0222:TIOASO>2.0.CO;2.

McKee, T. B., N. J. Doesken, and J. Kleist, 1993: The relationship of drought frequency and duration to time scales. Proc. Eighth Conf. Applied Climatology, Anaheim, CA, Amer. Meteor. Soc., 179–184.

Meyer, S. J., K. B. Hubbard, and D. A. White, 1993a: A crop-specific drought index for corn: I. Model development and validation. *Agron. J.*, **85**, 388–395, https://doi.org/10.2134/agronj1993.00021962008500020040x.

——, ——, and ——, 1993b: A crop-specific drought index for corn: II. Application in drought monitoring and assessment. *Agron. J.*, **85**, 396–399, https://doi.org/10.2134/agronj1993.00021962008500020041x.

Moorhead, J. E., P. Gowda, D. Porter, T. Howell, V. Singh, and B. Stewart, 2013: Use of crop-specific indices for determining irrigation demand in the Texas high plains. *Appl. Eng. Agric.*, **29**, 905–916, https://doi.org/10.13031/aea.29.10201.

NASS, 2020a: Quick stats. National Agricultural Statistic Service, U.S. Department of Agriculture, https://www.nass.usda.gov/Quick_Stats/Lite/.

NASS, 2020b: Charts and maps. National Agricultural Statistic Service, U.S. Department of Agriculture, https://www.nass.usda.gov/Charts_and_Maps/Field_Crops/index.php.

NCEI, 2020: Regional climate centers. National Oceanic and Atmospheric Administration, https://www.ncdc.noaa.gov/customer-support/partnerships/regional-climate-centers.

North Dakota Agricultural Weather Network Center, 2020: Corn Growing Degree Days (GDD), Department of Agriculture, North Dakota State University, accessed 9 March 2020, https://ndawn.ndsu.nodak.edu/help-corn-growing-degree-days.html.

Otkin, J. A., M. C. Anderson, C. Hain, I. E. Mladenova, J. B. Basara, and M. Svoboda, 2013: Examining rapid onset drought development using the thermal infrared–based evaporative stress index. *J. Hydrometeor.*, **14**, 1057–1074, https://doi.org/10.1175/JHM-D-12-0144.1.

——, M. Svoboda, E. D. Hunt, T. W. Ford, M. C. Anderson, C. Hain, and J. B. Basara, 2018: Flash droughts: A review and assessment of the challenges imposed by rapid-onset droughts in the United States. *Bull. Amer. Meteor. Soc.*, **99**, 911–919, https://doi.org/10.1175/BAMS-D-17-0149.1.

Palmer, W. C., 1965: Meteorological drought. U.S. Weather Bureau Research Paper 45, 58 pp., http://www.ncdc.noaa.gov/temp-and-precip/drought/docs/palmer.pdf.

Pendergrass, A. G., and Coauthors, 2020: Flash droughts present a new challenge for subseasonal-to-seasonal prediction. *Nat. Climate Change*, **10**, 191–199, https://doi.org/10.1038/s41558-020-0709-0.

Perkins, S. E., and L. V. Alexander, 2013: On the measurement of heat waves. *J. Climate*, **26**, 4500–4517, https://doi.org/10.1175/JCLI-D-12-00383.1.

Quiring, S. M., J. Lucido, L. Winslow, T. Ford, B. Bijoy Baruah, J. Verdin, R. Pulwarty, and M. Strobel, 2015: Development of a coordinated National Soil Moisture Network: A pilot study. *2015 Fall Meeting*, San Francisco, CA, Amer. Geophys. Union, Abstract IN41B-1704.

Rangwala, I., L. L. Smith, G. Senay, J. Barsugli, S. Kagone, and M. T. Hobbins, 2019: Landscape Evaporative Response Index (LERI): A high resolution monitoring and assessment of evapotranspiration across the contiguous United States. U.S. Geological Survey ScienceBase, https://www.sciencebase.gov/catalog/item/5c8020d7e4b0938824459be9.

Redmond, K. T., 2002: The depiction of drought. *Bull. Amer. Meteor. Soc.*, **83**, 1143–1148, https://doi.org/10.1175/1520-0477-83.8.1143.

Reges, H. W., N. J. Doesken, J. Turner, N. Newman, A. Bergantino, and Z. Schwalbe, 2016: CoCoRaHS: The evolution and accomplishments of a volunteer rain gauge network. *Bull. Amer. Meteor. Soc.*, **97**, 1831–1846, https://doi.org/10.1175/BAMS-D-14-00213.1.

Rippey, B., 2019: 2018 Farm Bill and the USDM. *U.S. Drought Monitor Forum 2019*, Bowling Green, KY, Western Kentucky University, https://drought.unl.edu/archive/Documents/NDMC/Workshops/963/Pres/Rippey-2018%20Farm%20Bill%20and%20the%20USDM.pptx.

Rippey, B. R., 2015: The U.S. drought of 2012. *Wea. Climate Extremes*, **10**, 57–64, https://doi.org/10.1016/j.wace.2015.10.004.

Rui, H., and D. Mocko, 2019: README document for North American Land Data Assimilation System Phase 2 (NLDAS-2) Products. NASA, 44 pp., accessed 9 March 2020, https://hydro1.gesdisc.eosdis.nasa.gov/data/NLDAS/README.NLDAS2.pdf.

Schaefer, G. L., M. H. Cosh, and T. J. Jackson, 2007: The USDA natural resources conservation service Soil Climate Analysis Network (SCAN). *J. Atmos. Oceanic Technol.*, **24**, 2073–2077, https://doi.org/10.1175/2007JTECHA930.1.

Schubert, S. D., M. J. Suarez, P. J. Pegion, R. D. Koster, and J. T. Bacmeister, 2004: On the cause of the 1930s Dust Bowl. *Science*, **303**, 1855–1859, https://doi.org/10.1126/science.1095048.

Scott, B. L., T. E. Ochsner, B. G. Illston, C. A. Fiebrich, J. B. Basara, and A. J. Sutherland, 2013: New soil property database improves Oklahoma Mesonet soil moisture estimates. *J. Atmos. Oceanic Technol.*, **30**, 2585–2595, https://doi.org/10.1175/JTECH-D-13-00084.1.

Seager, R., J. Feldman, N. Lis, M. Ting, A. P. Williams, J. Nakamura, H. Liu, and N. Henderson, 2018: Whither the 100th Meridian? The once and future physical and human geography of America's arid–humid divide. Part II: The meridian moves east. *Earth Interact.*, **22**, https://doi.org/10.1175/EI-D-17-0012.1.

Selby, J., O. S. Dahi, C. Fröhlich, and M. Hulme, 2017: Climate change and the Syrian civil war revisited. *Polit. Geogr.*, **60**, 232–244, https://doi.org/10.1016/j.polgeo.2017.05.007.

Smith, A. B., 2020: Billion-dollar weather and climate disasters. NOAA/National Centers for Environmental Information, https://www.ncdc.noaa.gov/billions/.

Smith, K. H., M. Svoboda, M. Hayes, H. Reges, N. Doesken, K. Lackstrom, K. Dow, and A. Brennan, 2014: Local observers

fill in the details on drought impact reporter maps. *Bull. Amer. Meteor. Soc.*, **95**, 1659–1662, https://doi.org/10.1175/1520-0477-95.11.1659.

Smith, S., and B. Kurtz, 2015: Why do us corn yields increase? The contributions of genetics, agronomy, and policy instruments. *AgBioForum*, **18**, 297–302, https://doi.org/10.1007/978-3-319-67958-7_6.

Sousa, P. M., R. C. Blamey, C. J. Reason, A. M. Ramos, and R. M. Trigo, 2018: The 'Day Zero' Cape Town drought and the poleward migration of moisture corridors. *Environ. Res. Lett.*, **13**, 124025, https://doi.org/10.1088/1748-9326/aaebc7.

Svoboda, M., and B. Fuchs, 2016: Handbook of drought indicators and indices. WMO-1173, World Meteorological Organization, 45 pp., https://public.wmo.int/en/resources/library/handbook-of-drought-indicators-and-indices.

Trenberth, K. A., G. Dai, G. van der Schrier, P. D. Jones, J. Barichivich, and K. R. Biffa, and J. Sheffield 2014: Global warming and changes in drought. *Nat. Climate Change*, **4**, 17–22, https://doi.org/10.1038/nclimate2067.

Udall, B., and J. Overpeck, 2017: The twenty-first century Colorado River hot drought and implications for the future. *Water Resour. Res.*, **53**, 2404–2418, https://doi.org/10.1002/2016WR019638.

USBR, 2020: AgriMet crop coefficients. Accessed 9 March 2020, https://www.usbr.gov/pn/agrimet/cropcurves/crop_curves.html.

Vins, H., J. Bell, S. Saha, and J. J. Hess, 2015: The mental health outcomes of drought: A systematic review and causal process diagram. *Int. J. Environ. Res. Public Health*, **12**, 13 251–13 275, https://doi.org/10.3390/ijerph121013251.

Wei, J. F., and P. A. Dirmeyer, 2012: Dissecting soil moisture-precipitation coupling. *Geophys. Res. Lett.*, **39**, L19711, https://doi.org/10.1029/2012GL053038.

Wilhite, D., R. Pulwarty, K. Jacobs, and R. Dole, 2005: The hardest working river: Drought and critical water problems in the Colorado River Basin. *Drought and Water Crises: Science, Technology, and Management*, D. Wilhite, Ed., CRC Press, 249–285.

Xia, Y., C. D. Peter-Lidard, M. Huang, H. Wei, and M. Ek, 2014: Improved NLDAS-2 Noah-simulated hydrometeorological products with an interim run. *Hydrol. Processes*, **29**, 780–792, https://doi.org/10.1002/hyp.10190.

Yuan, Y., M. Pan, H. Beck, C. Fisher, R. E. Beighley, S. Kao, Y. Hong, and E. Wood, 2019: Calibrated VIC model parameters over CONUS. *Water Resour. Res.*, **55**, 7784–7803, https://doi.org/10.1029/2018WR024178.